A FEASIBILITY STUDY OF A DIAGNOSTIC SYSTEM FOR JET USING LASER EXCITED LYMAN α FLUORESCENCE TO MEASURE ATOMIC HYDROGEN DENSITIES

(Jet-Design-Study 14.3)

K.-H. Steuer, H. Röhr, P. Bogen[+], R.W. Dreyfus[++]

IPP III/101 May 1985

MAX-PLANCK-INSTITUT FÜR PLASMAPHYSIK

8046 GARCHING BEI MÜNCHEN

MAX-PLANCK-INSTITUT FÜR PLASMAPHYSIK

GARCHING BEI MÜNCHEN

A FEASIBILITY STUDY OF A DIAGNOSTIC SYSTEM FOR JET USING LASER EXCITED LYMAN α FLUORESCENCE TO MEASURE ATOMIC HYDROGEN DENSITIES

(Jet-Design-Study 14.3)

K.-H. Steuer, H. Röhr, P. Bogen[+], R.W. Dreyfus[++]

IPP III/101 May 1985

Die nachstehende Arbeit wurde im Rahmen des Vertrages zwischen dem Max-Planck-Institut für Plasmaphysik und der Europäischen Atomgemeinschaft über die Zusammenarbeit auf dem Gebiete der Plasmaphysik durchgeführt.

CONTENTS

IPP III/101

K.-H. Steuer
H. Röhr
P. Bogen[+]
R.W. Dreyfus[++]

A FEASIBILITY STUDY OF A DIAGNOSTIC SYSTEM FOR JET USING LASER EXCITED LYMAN α FLUORESCENCE TO MEASURE ATOMIC HYDROGEN DENSITIES

(JET-Design-Study 14.3)

(May 1985)

Summary

This report discusses the possibility of using Lyman-α fluorescence diagnostics in large tokamaks (i.e. JET) to determine the neutral gas density and temperature. Spatially resolved measurements of the neutral hydrogen atom density profile are needed in order to understand plasma energy balance and procession of recycling and particle diffusion. Neutral hydrogen density measurements are possible if high-power lasers at 121,6 nm are available. Therefore this study is more a status report on the feasibility of Lyman-α lasers than a detailed design proposal for a possible layout of a measuring system in a tokamak. Although very intensive efforts have been invested in the development of Lyman-α lasers at various laboratories for quite some time, no suitable laser system meeting the power and linewidth requirements is yet available. Frequency-tripled lasers are at present just capable of entering the power range in which it should be posible to measure the boundary density in tokamaks. These lasers are not expected to afford any major power increase, and so the measurements will likely be restricted exclusively to the boundary region.

A measuring system in a tokamak using a frequency-tripled laser, however, is not yet in operation. A scattering system has been completely installed in ASDEX and first results from cleaning discharges have been obtained. It has been found that improvements must be incorporated before reliable results can be expected from the edge of the main plasma. This report gives a detailed account of the experience that has been gained in ASDEX with this system.

[+] Institut für Plasmaphysik, Assoc. Euratom
Kernforschungsanlage 5170 Jülich, Germany

[++] IBM Thomas J. Watson, Research Center,
Yorktown Heights, New York 10589

The results show that the improvements envisaged should allow detection of boundary densities in the region of 10^{10} particles/cm^3, provided the temperatues are not much in excess of 10 eV.

It would be even more interesting to measure the neutral gas density profile right to the centre of the plasma, i.e. down to densities of 10^7 particles/cm^3 at temperatues of about 1 keV. This calls for laser powers about 2 to 3 orders of magnitude above those attainable with frequency tripling. This requires new developments of powerful VUV lasers. A promising way appeared to be the argon excimer laser, which has a broad fluorescence spectrum (Lyman α being present within its half-width) and which emits reproducible powers of a few 100 kW at its central wavelength of 126.1 nm. The laser was tuned to 123.2 nm, but it could not be tuned at the moment to even shorter wavelengths owing to:

1. enhanced absorption of the VUV radiation by excited argon atoms and excimers, which reduce the gain at Lyman α to very low values and
2. problems due to destruction of optical layers by super-radiance.

The results of our investigations on tuning of the argon excimer laser are briefly described in this report. A detailed description of the results is published in IPP-report 1/186.

In view of our experience with the argon excimer laser we come to the conclusion that direct intracavity tuning to Lyman α is not possible. Therefore we investigate the possibility of tuning the laser not within the resonator but outside, by means of the stimulated Raman effect. The first anti-Stokes line in deuterium is located exactly at Lyman α. A commercially available ArF-laser (193 nm) was used to study the stimulated Raman effect in different gases (H_2, D_2, CH_4). The results indicate that the minimum luminosities required for shifiting the Ar_2^*-laser in deuterium exceeds those presently achievable. The results and requirements are described in IPP-report III/89.

1. Significance of neutral gas density measurement

The electron density in a tokamak is the result of two competing processes. On the one hand, there is continual loss of charged particles as a result of diffusion to the wall; on the other, neutral gas enters the plasma, and is ionized. To maintain stationary condition, the electrons lost have to be continually replaced by ionization of neutral hydrogen in the plasma (recycling). If the ionization rate as a function of radius is known, it is possible to determine the particle confinement time or particle diffusion coefficient as a function of radius. As the ionization rate is proportional to the electron and neutral gas densities, the source term can only be given locally if the neutral gas density profile is known in addition to the electron density profile, which is generally measured by Thomson scattering.

Furthermore, knowing the quantity $n_o(r)$ one can treat the question of the penetration depth of the neutral hydrogen puffed in and the concomitant question of high-density tokamak plasma build-up. To determine whether the electron density rise in the interior is caused by a high source term or by strong inward diffusion of charged particles, the neutral gas density has to be known particularly in the central region.

Spatially resolved mesurements of the neutral hydrogen atom density therefore are needed in order to clarify considerably the important role of neutrals in energy and particle balance of fusion plasmas in recycling of hydrogen isotopes between plasma and vacuum walls and in the operation of neutral beam injectors, gas puffing and pellet injection.

2. Previous measuring methods

By spectroscopic methods it is only possible to deal with excited hydrogen atoms. These methods are indirect since population models have to be used in order to calculate back from the population of a higher quantum state to the much higher total number of atoms in the ground state. The use of such models is particularly debatable when radiation reabsorption also occurs, as is the case with large and/or dense plasmas. Furthermore, spectroscopic methods yield values averaged over the plasma volume. As in particular the atoms in the boundary region radiate, spatial resolution is a problem.

Another method of determining the neutral gas density is passive neutral particle analysis. This consists in assuming a plausible n_o profile (e.g. with the help of monte-carlo calculations) and calculating back to the total number of hydrogen atoms from the number of high-energy charge exchange neutrals of given energy that make their way outwards. This method, which has been very successful in present-day tokamaks, is also only conditionally applicable to the plasma interior in large devices, since just a small fraction of the central charge exchange neutrals make their way outwards. In active neutral particle analysis a hydrogen beam fired into the plasma enhances the hydrogen concentration in the centre. This increases the charge exchange rate and facilitates detection. This method also suffers from low permeability of the plasma to neutrals.

3. Resonance scattering

Resonance fluorescence may be used for spatially resolved measurement of the neutral gas density. As most of the hydrogen atoms in the plasma are in the ground state, a VUV light source at Lyman alpha (121,6 nm) is required for excitation. When irradiated with Lyman alpha light, the hydrogen atom is converted to the first excited state n = 2. Within approximately 2.1 ns the atoms spontaneously return to the ground state, emitting a Lyman alpha quantum. This light is measured as scattered light in resonance fluorescence.

Fluorescence spectroscopy offers better spatial resolution and the interpretation can be made independent of the plasma density and temperature. The main difficulty is to find sufficiently strong light sources.

Unlike the scattering intensity attainable in Thomson scattering the resonance scattering may be saturated. Whereas the scattering intensity with weak sources remains proportional to the exciting intensity, a sufficiently intense source leads to equal population of the atomic energy levels considering the statistical weights. If the upper level is saturated, the atom emits corresponding to its spontaneous transition rate A_{21} independently of the intensity of the source.

In the following section it is estimated what VUV powers are necessary for a Lyman alpha scattering experiment in a tokamak.

4. Performance of the Lyman alpha source

4.1 Estimation of the S/N ratio

Figure 1 shows a diagram of the scattering geometry, on which the following estimates are based. Light from the Lyman alpha source is focused with a VUV lens on a surface which, for simplicity, is assumed to be a square with side length q. The observation system, placed at 90° and covering the solid angle Ω_s, sees only part of the plasma volume irradiated by the source, viz the scattering volume V_s with the cross-sectional area F_s. A filter, e.g. a Lyman alpha interference filter, separates the light in the desired spectral range. Preference should be given to a Lyman alpha interference filter over a VUV grating monochromator because of its high permeability ($T \approx 15$ to 20 %). The scattered light finally impinges on a solar blind photomultiplier, where it is converted into photoelectrons. The combined efficiency of the imaging system, filter and photomultiplier has the value η.

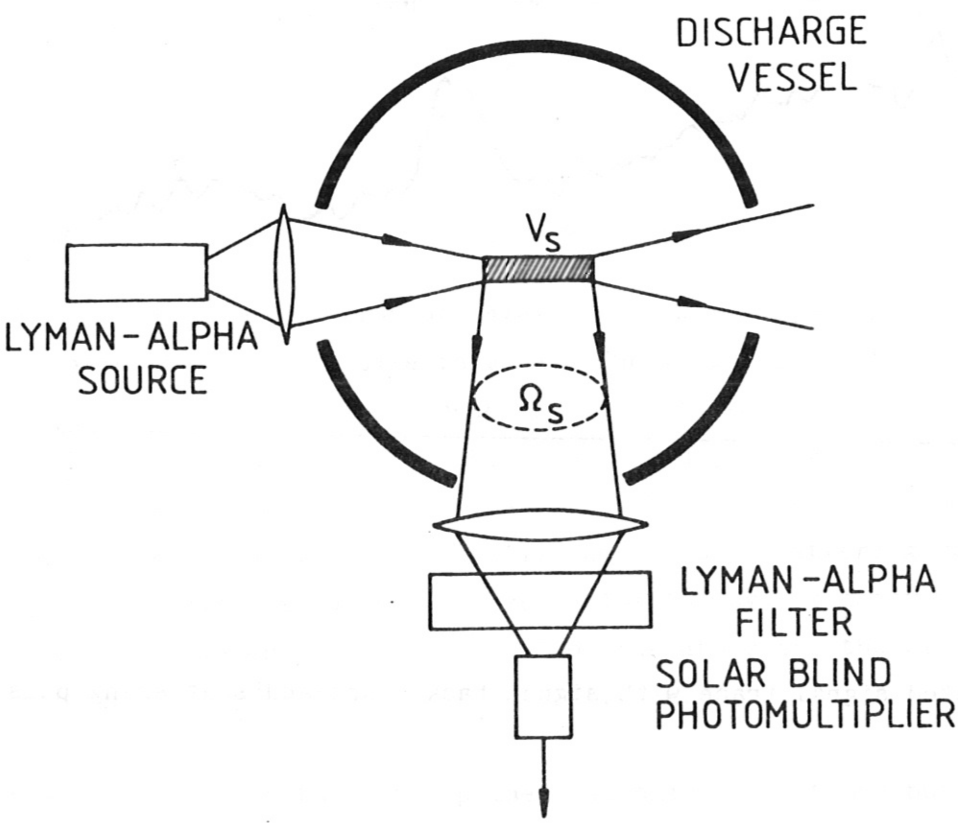

Fig. 1 Schema of scattering apparatus

Figure 2 shows a signal trace expected on the oscilloscope screen. The laser is switched on during the time Δt. The spontaneous emission of the plasma in and outside the scattering volume causes a high signal background. To detect a scattering signal, it has to be larger than the background noise. The measuring accuracy is governed by the signal-to-noise ratio. The noise of the background signal can have two reasons.

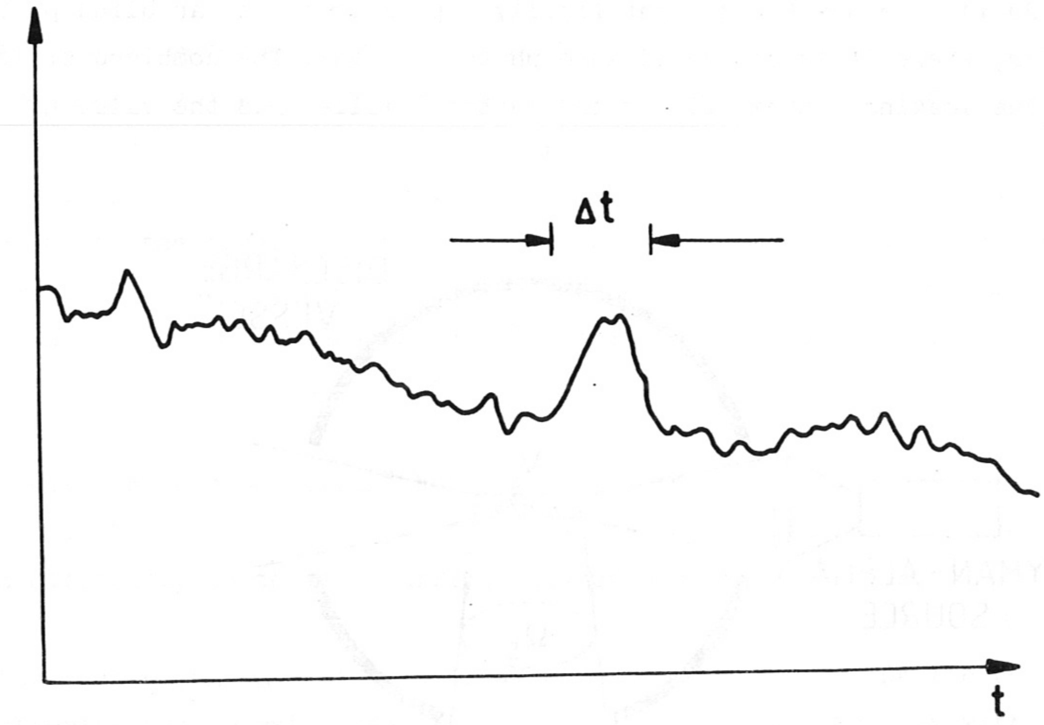

Fig. 2 Expected signal trace with signal background and scattering pulse.

Firstly, it may be due to fluctuations in the intensity of the plasma emision as a result of fluctuations in the electron density or temperature. Secondly, it is due to the shot noise of the detector. If N_u photoelectrons are emitted from the cathode of the photomultiplier within a time Δt, the fluctuation of this number (and hence of the signal) is at least $\pm(N_u)^{1/2}$ for statistical reasons. The highest detection sensitivity is achieved when the time resolution of the detector system agrees with the length of the scattering signal. This case serves as the basis for the following estimates.

With B denoting the plasma luminosity (dimension: photons cm^{-2} s^{-1} $sterad^{-1}$) in the spectral range in which the detector system is sensitive the number of photoelectrons released by plasma emission in the time Δt is

$$N_U \approx \eta B \, F_s \Omega_s \, \Delta t \qquad (1)$$

where F_s and Ω_s are the cross-sectional areas of the scattering volume covered by the detector system and the solid angle, respectively. The noise of the signal is $\pm(N_u)^{1/2}$. The number of photoelectrons released by Lyman alpha resonance scattering is given by

$$N_s = A_{21} \, (N_2 - N_2^0) \, V_s \frac{\Omega_s}{4\pi} \eta \Delta t \qquad (2)$$

where N_2 is the population of level 2 during the laser pulse, and N_2^o the population before this time interval. The variation of the level populations due to irradiation is described by rate equations. As the collision limit for a tokamak plasma is between levels 3 and 4, the collision coupling of level 2 to the higher states can be neglected. Furthermore, the weak excitation of level 2 by collisions in the scattering volume will be negligible relative to the intense excitation by the laser beam. Before the start of the laser pulse almost all of the atoms are therefore in the ground state: $N_1^o \neq 0$, $N_2^o = N_4 = \dots . = 0$.

After the start of the laser pulse stationary conditions build up within a time roughly equivalent to the inverse of the spontaneous transition rate A_{21}. With Lyman alpha this is the case after 2 ns. The rate equation for levels 1 and 2 is:

$$N_1 B_{12} I_L = N_2 B_{21} I_L + N_2 \, A_{21} \qquad (3)$$

where B_{12} and B_{21} are the Einstein coefficients for stimulated absorption and emission, and I_L is the laser intensity/Å. Because of the initial condition it also holds that

$$N_1 + N_2 = N_1^o \tag{4}$$

From eq. (3) it follows directly that

$$N_2 = \frac{B_{12} I_L N_1}{B_{21} I_L + A_{21}} \tag{5}$$

With the Einstein relations

$$g_2 B_{21} = g_1 B_{12} \tag{6}$$

$$\frac{\hbar \omega^3}{\pi^2 c^3} B_{21} = A_{21} \tag{7}$$

one then obtains

$$N_2 = \frac{(g_2/g_1)\ I_L\ N_1}{I_L + A_{21}/B_{21}} \tag{8}$$

Equation (4) then yields the population N_2, which governs the size of the scattering signal, as a function of the total neutral particle density N_1^o:

$$N_2 = \frac{g_2/g_1\ I_L}{((g_1 + g_2)/g_1) I_L + A_{21}/B_{21}}\ N_1^o \tag{9}$$

The saturation intensity I_{sat} is defined as the spectral laser intensity at which the excited level decays equally as a result of stimulated and spontaneous emission:

$$B_{21}\ I_{SAT} = A_{21} \tag{10}$$

For Lyman alpha one obtains with eq. (7)

$$I_{SAT} = 560 \frac{kW}{\AA\ cm^2}$$

With eq. (10) for eq. (9) becomes

$$N_2 = \frac{g_2/g_1\ I_L}{((g_1 + g_2)/g_1)I_L + I_{SAT}}\ N_1^o \tag{11}$$

Two limiting cases can be distinguished:

a) Weak excitation: $I_L \ll I_{SAT}$

For the population of level 2 as a function of the laser intensity one obtains

$$N_2 = \frac{g_2\ I_L}{g_1\ I_{SAT}}\ N_1^o \tag{12}$$

The measured scattering intensity is proportional to $N_1^{\ o}$ and to the laser intensity.

b) Strong excitation: $I_L \gg I_{SAT}$

The laser radiation leads to saturation of the transition. The population in the excited level, and hence the scattering intensity, is independent of the laser intensity

$$N_2 = \frac{g_2}{g_1 + g_2}\ N_1^{\ o} \tag{13}$$

This yields altogether for the signal-to-noise ratio

a) with weak excitation (eqs. (1), (2), (12))

$$\frac{S}{N} = \frac{N_S}{\sqrt{N_U}} = \frac{A_{21}(g_2/g_1)(I_L/I_{SAT})N_1^{\ o}\ V_s\sqrt{\Omega_s\eta\Delta t}}{4\pi\ \sqrt{BF_s}} \tag{14}$$

b) with strong excitation (eqs. (1), (2), (13))

$$\frac{S}{N} = \frac{(g_2/(g_1+g_2))N_1^o \, V_s \sqrt{\Omega_s}\eta\Delta t}{4\pi\sqrt{BF_s}} \qquad (15)$$

For Lyman alpha one has $g_1 = 2$, $g_2 = 8$.

In order to excite all hydrogen atoms in the scattering volume, irradiation has to be applied over the entire Doppler width of the Lyman alpha transition. At a temperature of the H atoms of 1 keV the (full) Doppler width is:

for hydrogen 3.2 Å,
for deuterium 2.3 Å.

The source should thus have a spectral width of about 5 Å. The total laser intensity is then

$$P_L = I_L \Delta\lambda_D$$

To examine the signal and background levels expected for resonant scattering of Lyman α in fusion plasmas, it is necessary to know something about the magnitude and radial variation of the plasma parameters n_e, T_e, n_o. We have done 1D simulation calculations for JET with the Baldur-Code. Figure 3 shows radial profiles of T_e, T_i, n_o, and n_e at the end of a 5 sec heating phase with 30 MW neutral injection power /1/. The neutral gas profile is averaged over the torus and will certainly be different in the neighbourhood of strong particle sources e.g. limiter or valves.

The neutral gas density drops down from 10^{10} particles/cm^3 at the plasma limiter to about 10^6 in the plasma centre. The main decrease occurs within a length of about 30 cm.

Over the expected range of T_e, the excitation rate X_{12} of hydrogen by collisions is a slowly varying function, and consequently the integrated background Lyman α emission is more strongly dependent on the behaviour of $n_e(r)$ and $n_o(r)$, both of which have poorly defined values and steep gradients in the region of greatest contribution near the plasma limiter.

From the profiles we estimate a Lyman α background light in the range of 10^{15} photons/sec cm^2 sterad in agreement with estimations of Koopman et al. /2/ for TFTR. This figure will be the basis of the following estimates. As comparison, for example, at ASDEX we measured a Lyman α emission of 4.7 x 10^{14} photons/sec cm^2 sterad in divertor discharges and 1.4 x 10^{15} photons/sec^2 sterad in Ti-pumped divertor discharges.

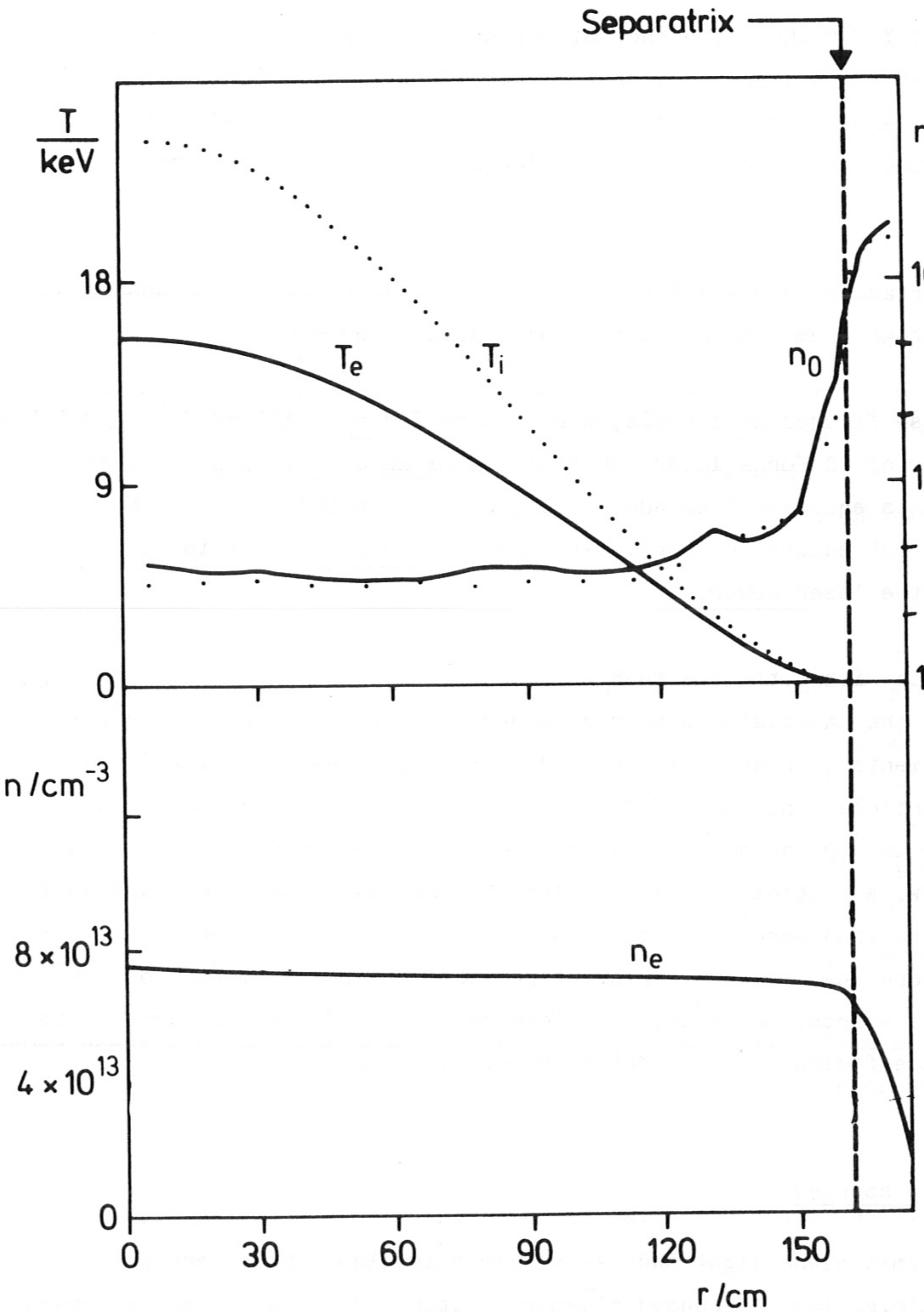

Fig. 3 1 D-simulation of a JET-plasma with the Baldur-code: radial profiles on T_e, T_i, n_o and n_e.

We assume a solid angle of about 10^{-2} sterad for observation. The assumed value $\eta = 1$ % for the efficiency of the detector system refers to a facility composed of an imaging concave mirror, interference filter and photomultiplier, which itself has a quantum efficiency of 20 %. The crucial loss occurs at the interference filter, which has a maximum transmission of just 15 %.

To ensure reasonable spatial resolution, the scattering volume should not be longer than 5 cm. The cross-sectional area is $q^2 \approx 0.5$ cm^2.

Taking these figures as a basis, one obtains for $n_o = 10^7$ cm^{-3} a signal-to-noise ratio of 10 for a laser power of 1.5 mW in a 5 ns pulse. The scattering signal is equivalent to 400 photoelectrons. In this case the scattering volume is just saturated. For lower laser powers the S/N ratio is proportional to the laser power.

A comparison with estimates such as recently published by Koopman et al. /2/ shows that the calculations presented here are possibly too pessimistic. For experiments such as DITE, PLT and TFTR Koopman has calculated that neutral particle densities of 10^7 cm^{-3} with signal-to-noise ratios of between 20 and 50 can already be measured with Lyman alpha intensities of 10 to 20 kW. A critical check revealed that Koopman's approach is identical to that described here, but that his assumptions are much more optimistic and therefore lead to less stringent requirements being imposed on the Lyman alpha source. The biggest difference is that Koopman assumes 10 times as high an efficiency of the detector system as we do.

4.2 Thermal sources

The only Lyman alpha light sources hitherto available have been thermal radiators, e.g. laser-produced plasmas (Breton and Papoular /3/) or spark plasmas (Bogen and Lie /4/). With such thermal sources it is possible to attain in the plasma typical values of 100 W/cm^2 Å for the spectral power density at L_α. These values are far below the saturation intensity of 560 kW/cm^2 Å, so that the scattered light is proportional to the incident light intensity.

If these Lyman alpha powers attainable with thermal sources are substituted in the formulae, it is found that a neutral gas density of at least

10^{11} cm^{-3} has to be present in the scattering volume to allow measurement with an S/N ratio of just one.

It thus follows that thermal sources cannot be considered for scattering from tokamaks.

4.3 Conclusions

Lyman alpha scattering is just as simple in principle as Thomson scattering. In order to measure the neutral particle density in the centre of a tokamak or low-beta plasma, one needs about 1 MW in 5 ns with a bandwidth of 5 Å around Lyman alpha. These estimates have been deliberately kept conservative. Improvements in the detector system can lower the detection limit by an order of magnitude (≙100 kW in 5 ns).

5. Production of intense Lyman α radiation by nonlinear processes

With coherent light sources in the visible it has recently become possible by means of optically nonlinear processes in rare gases and metal vapour-rare gas systems to gain access to the vacuum UV range beyond the absorption limit of nonlinear crystals at 200 nm. The high qualities afforded by coherent light sources in the visible, such as narrow line width, small divergence and wide tuning range, can be extended to the VUV range by frequency tripling and difference or sum frequency generation. The spectral power densities here are orders of magnitude higher than those of synchrotrons or those of thermal sources hitherto available for spectroscopy in the VUV.

Effective generation of the third harmonic calls for phase matching of the fundamental and harmonic waves in the non-linear system. This is achieved by exact setting of the partial pressures in a gas mixture if the refractive index of one gas is smaller at the 3rd harmonic than at the fundamental wavelength. The VUV radiation yield is essentially governed by the absorption cross-section of the nonlinear medium at these wavelengths. It is particularly large, however, for atoms with two-photon-resonant intermediate levels.

In order to investigate the feasibility of such a laser source for a scattering experiment on JET we made experiments with the aim to choose optically nonlinear systems suitable for producing intense Lyman α radiation, quantitatively investigate them and determine the maximum attainable conversion efficinecy. A detailed description of the results is given in IPP report 1/185.

Theoretical analysis of frequency tripling shows that beryllium atoms are ideally suited to Lyman alpha generation owing to the location of their energy levels. However, producing the necessary homogeneous vapour pressures involves major techical problems since liquid beryllium is very aggressive and beryllium dust highly toxic. For this reason krypton, which can be phase-matched with argon at 364.8 nm and 121.6 nm because of its dispersion, was used as nonlinear medium for most of the experimental investigations. The absence of two-photon resonance means, that the value of the nonlinear susceptibility $\chi_r^{(3)}$ (3 ω), which is decisive for conversion, is much smaller than for beryllium. Since, however, with non-resonant frequency tripling in krypton it is possible to work with much higher densities and laser intensities, the conversion efficiencies for the two media in the small-signal range are comparable.

The central process limiting conversion efficiency, in both resonant and non-resonant frequency tripling, is the destruction of phase matching at high input intensities. In the non-resonant case this is due to the intensity dependence of the refractive indices (Kerr effect).

For the limiting case of non-resonant frequency tripling an analytical approximation for focused light with allowance for the Kerr effect was derived which allows, on the one hand, experimental determination of the nonlinear susceptibilities of Kr and, on the other, optimization of the Kr/Ar system. Furthermore, the influence of intensity fluctuations on the third harmonic generation that is exerted by the multi-mode structure of the laser radiation was investigated. The calculation shows that conversion with the laser used here is a factor of 6 as high as that with a single-frequency laser of same power, and the relative fluctuations from shot to shot are smaller than 15 %.

All experiments which we performed in the laboratory were conducted with a frequency doubled, ruby-laser-pumped dye laser system which could be tuned between 362.3 and 367.3 nm. The values of the nonlinear susceptibilities of krypton could be determined to 5th order of the perturbation calculation from the density and intensity dependences of the Lyman alpha radiation generated in pure krypton. Hence it was possible to give the optimum value for the product of the density, intensity and confocal parameter in a Kr/Ar mixture. With allowance for pressure broadening of the Kr resonance line at 123.85nm the optimum Kr pressure is 1.5×10^3 torr. The density dependence of the threshold intensity for laser-induced gas breakdown leads to an intensity of 5×10^9 W/cm^2 in the focus. Figure 4 shows a typical phase matching curve for a Kr/Ar mixture at 5×10^9 W/cm^2, e.g. the conversion efficiency as a function of the pressure ratio $R = N_{Ar}/N_{Kr}$. The krypton pressure was 1.5×10^3 torr. The dotted lines are numerical results. With the laser system used in the laboratory this affords a maximum conversion of 10^{-4} at the optimum Kr/Ar mixture ratio of 2.7. At peak input intensities of 3 MW this is equivalent to a Lyman alpha power of 300 W or 2×10^{12} photons per 10 ns pulse.

The system used in the laboratory was only able to produce 1 laser shot per discharge, because the pump laser was a single pulse ruby laser. Interesting prospects were recently afforded by the development of powerful excimer/dye lasers with high repetition rate. Therefore we used such a laser combination for the application at ASDEX.

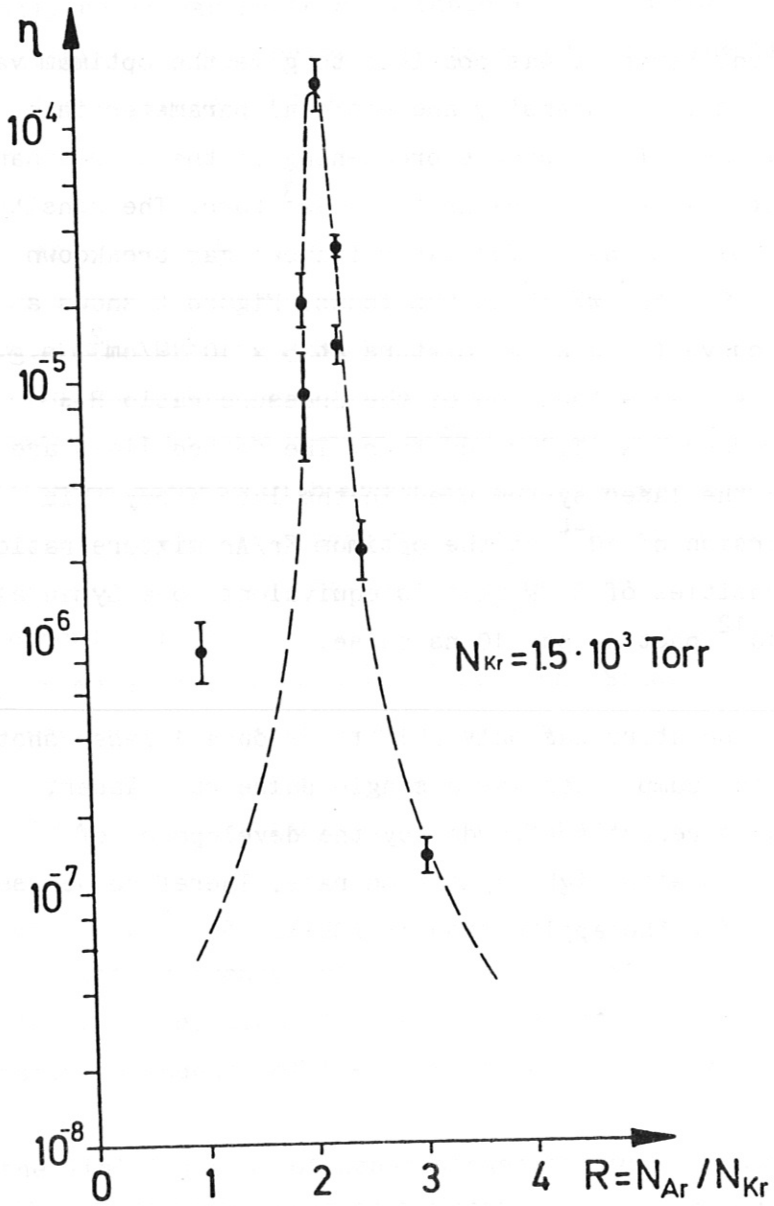

Fig. 4 Phase matching curves for a Kr/Ar mixture with the input intensity 5×10^9 W/cm^2 at the Kr pressure 1.5×10^3 torr.

6. Status of Lyman- Scattering from H Atoms Using a Frequency Tripled Laser

The resonance fluorescence system for measuring H-atom densities involved generating, scattering and detecting 121,6 nm photons. A scattering apparatus tested on ASDEX is a joint Max-Planck IPP-KFA, IPP/EURATOM project and is summarized in the following. The equipment operates essentially as expected, however, observation of Lyman-α scattering in ASDEX has been limited to D.C. and 50 Hz discharges. A primary reason of a limitation is the difficulty of optical alignment while the equipment is installed on ASDEX.

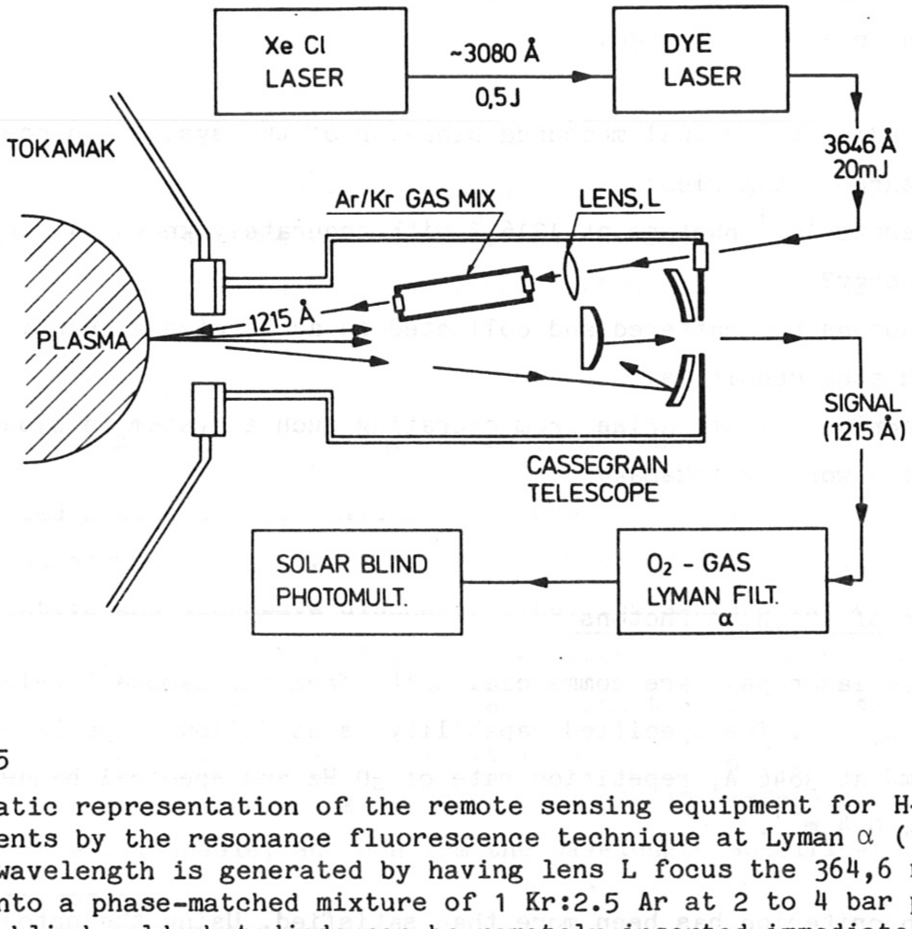

Fig. 5
Schematic representation of the remote sensing equipment for H-atom measurements by the resonance fluorescence technique at Lyman α (121,6 nm). This wavelength is generated by having lens L focus the 364,6 nm fundamental into a phase-matched mixture of 1 Kr:2.5 Ar at 2 to 4 bar pressure. A solar blind gold photodiode can be remotely inserted immediately after the tripling gas cell in order to accurately establish the VUV power. The telescope is 30 cm dia and 2.5 m long in order to remove the photomultiplier from the plasma, magnetic fields and X-rays originating in a tokamak.

Figure 5 gives a schematic view of the system as it was installed on the ASDEX Tokamak. The description will follow the same sequence as one of the nanosecond pulses travels through the apparatus. First, an excimer/dye laser pair generates up to 3 M Watt of tunable 364,6 nm radiation. Lens L focuses this energy into a Kr:Ar gas mixture held at 2 to 4 atmospheres. The nonlinear optical behavior of this mixture Kr:Ar (1 : 2.5) generates third harmonic radiation near 121,6 nm with a power efficiency of up to 10^{-5}; which means $\lesssim 10^{11}$ photons at 121,6 nm.

These 10^{11} photons excite hydrogen in observed volume of 1 cm^2 x 5 cm at radial position 0 to 40 cm inside the ASDEX vessel. About 0.1 % of the H-atoms in this volume are excited when their kinetic energy is 40 eV. With a H-atom density of 10^{10} cm^{-3}, 5 x 10^7 Lyman-α photons are scattered into 4π. The present 30 cm dia telescope collects 5 x 10^{-4} of these photons. Optical losses in the telescope reduce this pulse to 3.8 x 10^3 photons or 570 photoelectrons in the photomultiplier. The last number is particularly important later because it must override background noise signals arising purely from the plasma discharge.

Questions regarding the actual measured behavior of the system can now be divided into three categories:

- Can one generate 10^{11} photons at 1216 Å with accurately known wavelength and total energy?
- Can these photons be scattered and collected so as to give a quantitative measure of H-atom densities?
- What interferring effects arise from operating such a system in close proximity to a working tokamak?

6.1 Generating of 121,6 nm Photons

The excimer/dye laser pair are commercial units from the Lambda Physics Corp. Göttingen, FRG. The specified capability is as follows: dye laser output of 16 mJ at 3646 Å, repetition rate of 30 Hz and spectral bandwidth of 50 mÅ, i.e. 0.4 m^{-1}.

The wavelength criterion has been more than satisfied. Using the optogalvanic effect in a hollow cathode argon discharge the calibration is corrected to within ±20 mÅ (~0.15 cm^{-1}). This implies an accuracy of better than ±7 mÅ (~0.5 cm^{-1}) at 121,6 nm. For comparison, one might note that the Lyman-α line width at room temprature is 1 cm^{-1}. The present calibration therefore implies an absolute velocity measurement to better than 10^5/sec. The short time wavelength stability is about twice as accurate as above, hence recative velocity profiles can be measured to effectivly << 100 K.

Needless to say this accuracy exceeds the requirements for using this system on tokamak plasmas. In fact, the excitation peaks of H and D will be distinguishable up to an atom energy of ~10 eV.

Harmonic conversion of 364,6 nm power to 121,6 nm operates satisfactorily within some qualifying limitations. If one tries to obtain $\gg 10^{11}$ photons, then either one cannot operate at 30 Hz/or the rate of damages of components is too high and the system is not reliable.

The dye laser output is converted to 121,6 nm within the Kr/Ar gas mixture. Establishing good phase matching at a particular wavelength means that the mixture ratio must be correct to ±0.5 %. The output power and energy at Lyman α have been calibrated using both a photoionization chamber and photo-diodes.

The conclusion of this section is that 10^{11} photons at Lyman-α can indeed be generated with calibrated wavelength and energy. The one qualifying fact is that significant service and repair time are required if one pushes to this energy while simultaneously using a repetition rate of 10 - 30 Hz.

6.2 Scattering and Collection of 121,6 nm Photons in the Laboratory

Calibrated H-atom sources have been successfully used with the optical apparatus shown in Fig. 5. These sources were of both the thermally dissociative and microwave discharge type. The appearances of the signals in fluorscence are shown in Fig. 6. The fitted curves show the theoretical line shape anticipated for 300° K D-atoms and the present laser line width. The D-atom mean velocity is about 1.5×10^{5} cm/sec. It is evident that Doppler shifts corresponding to velocities of $<10^{5}$ cm/sec, i.e. 100°K energy, are measurable, and confirm the wavelength specifications given in the last section.

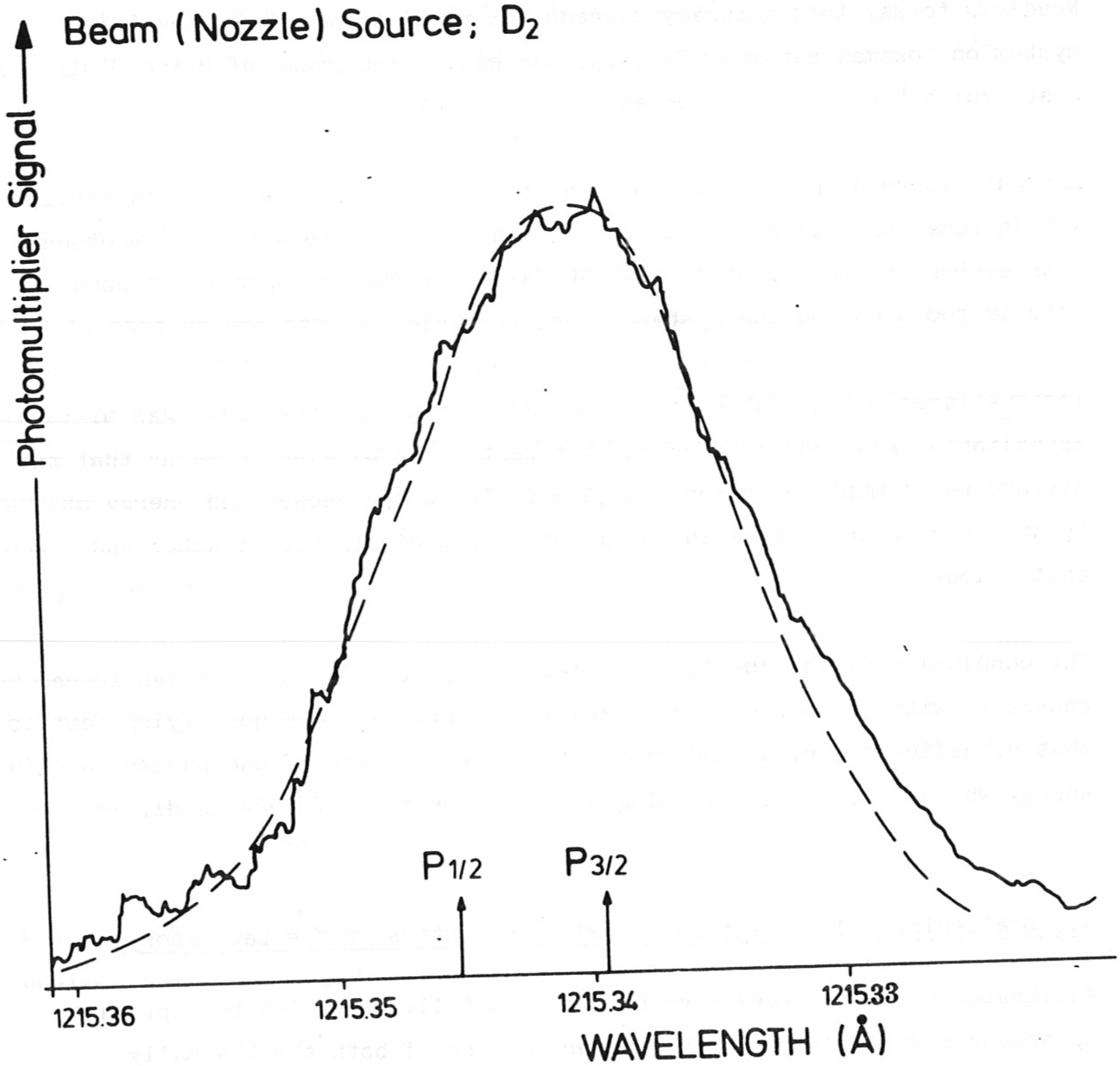

Fig. 6 Lyman-α fluorescence signal from room temperature D atoms. Dashed curve normalized to maximum signal.

As outlined in the introduction, the photomultiplier output can be estimated on the basis of the input Lyman-α energy. Results, such as Fig. 6, indicate that the optical system is operating at ~70 % of calculated sensitivity. This is a reasonable demonstration that the overall optical behavior approaches quite closely to the design parameters.

With respect to the above measurements, the minimum detectable H-atom concentration is set by the background stray light. The light comes from both the 3646 Å and 1216 Å radiation scattering of the vessel walls and then subsequently striking the PMT cathode. The solar blind photomultipliers, particularly, with KBr photocathodes, discriminate strongly against the UV component; however, the latter's 10^5 times higher power (over the VUV) essentially cancels out this discrimination ratio. Part of the stray light existed because only a single optical baffle was utilized. In comparison to this situation, the installation on ASDEX has a very efficient beam dump plus the benefit of the large vacuum chamber. Under these improved conditions, less than 1 photon of stray light was detected per shot. The detectability of H atoms (at 300^oK) is then calculated to be $\sim 10^6$ cm^{-3} and indicates the high sensitivity of the present technique.

6.3 Lyman-α Scattering in ASDEX

The optical system was installed on the ASDEX Tokamak. The signals from the 10 A and 0.6 kA cleaning discharges are shown in Fig. 7.

As is to be expected, the observed line widths and hence H-atom temperatures differ noticeably. The densities and temperatures are still slightly below the generally expected values for these discharges.

Corrective steps are underway to improve the alignment possibilities, these involve both removable and fluorescent targets that will check the optical path at various points. The most critical points (second to the crossing point of the telescope and laser axes which is not readily accessible) is the exit window of the high pressure gas cell and the beam dump behind on the inner wall of ASDEX. After the improvements we will try to measure densities and temperatures at the plasma edge in main discharges.

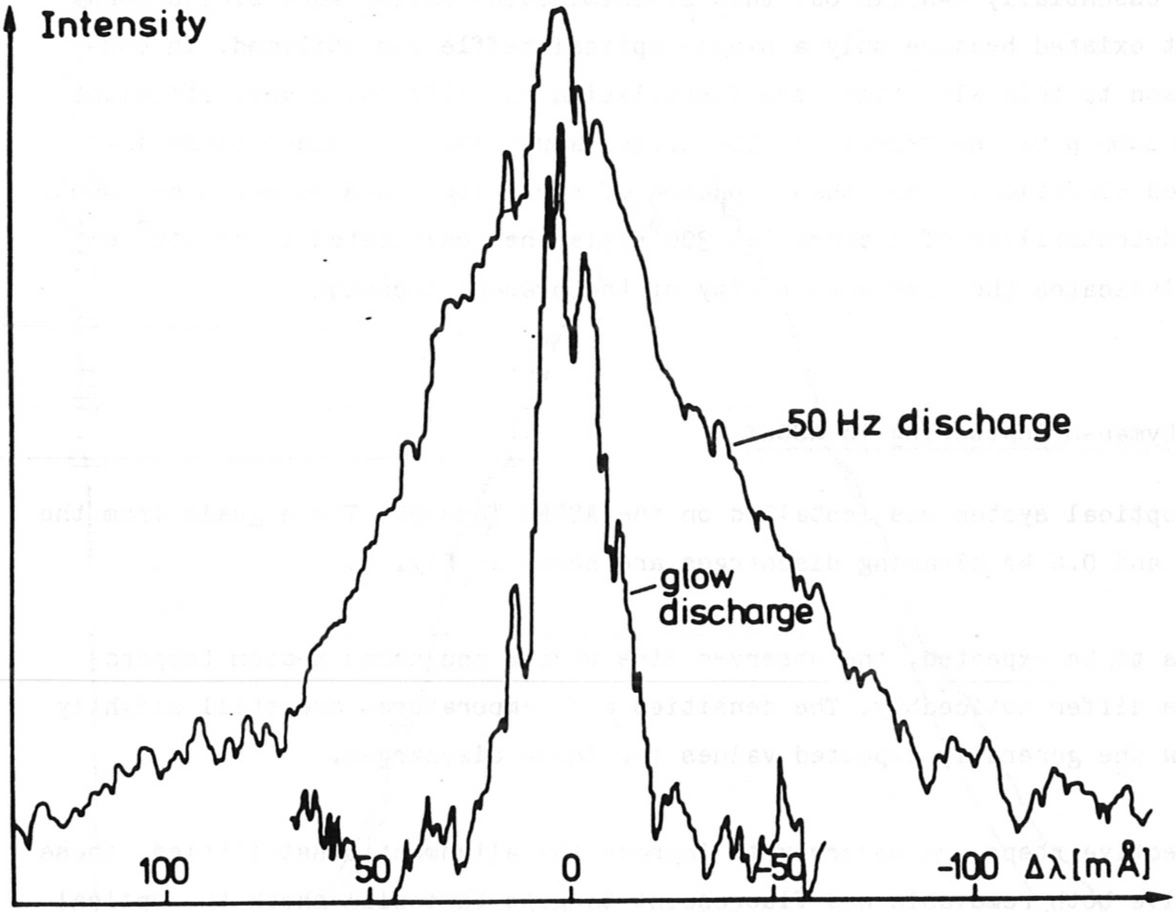

Fig. 7 The resonance fluorescence signal obtained with a low current ~10 A, glow discharge and an intermediate (~1 kA) current, 50 Hz discharge. Note the increased current has produced a 3.5 times broader Doppler profile.

One complicating effect was the absorption of Lyman-α light by H-atoms within the telescope. If the surface recombination coefficient for 2H → H_2 is very low, then the self absorption in the Cassegrain telescope may be in the range of e^{-2} to e^{-20} on line center. Of course, in discharges other than the 10 A glow discharge, the broad fluorescence line primarily will bypass the narrow 300° K absorption lines.

Several techniques have, so far, helped circumvent losses due to possible self absorption. First, in the laboratory source, differential pumping kept the Cassegrain H-atom density below ~10^8 cm^{-3}. Because of the different geometry with ASDEX as compared to the laboratory, differential pumping would not be as effective. In the case of ASDEX cleaning discharges, the solution was to flow the hydrogen supply gas through the telescope and from there into ASDEX. This simply swept the H atoms from the discharge away from the optical path within the telescope. A combination of the above solutions may be helpful in the case of high current ASDEX shots.

Quite possibly some effects from H atom absorption have already been observed. Measurements of Lyman-α light from the discharge give intensities of 10^{14} photons/sr x sec x cm^2, which is about 5 times lower than the quoted value. While mirror losses greater than 50 %/reflection and low photomultiplier response may account for a part of the reduction, self absorption may account for a finite fraction also.

The X-ray background was found to be not serious ($\ll$0.3 photoelectrons/shot) with 3 cm of lead shielding protecting the photomultiplier, P.M.T. A cadmium tube around the P.M.T. reduced the secondary effects from the Pb X-ray fluorescence emission.

The magnetic field during ASDEX discharges had negligible (30 %) effect upon the P.M.T. gain. Magnetic isolation was provided both by the 2.5 m length of the telescope and metal shielding as noted.

The resultant photomultiplier signal indicates ~60 photoelectrons are emitted within the 5 nsec response time of the detection system. The most important quantity is the shot noise due to these background photoelectrons, e.g. just about 8 photoelectrons. The latter number is to be compared to the 570 photoelectrons possibly being scattered from the third harmonic light.

The present status is to try to understand why these 570 photoelectrons were not observed. The answer seems to be a combination of several factors. To show the possible relative importance of each factor, we will consider a worst-case situation for each. The self absorption described above may be a reduction of one order of magnitude. Second, the third harmonic pulse was commonly 10^{10} photons and not 10^{11}. (The latter being only obtainable under marginal stability conditions). It is clear that any inaccuracy in alignment could decrease this signal well below the 8 photoelectrons of shot noise. While this can explain the lack of observed fluorescence, it should be recalled that the present series of tests is only an initial trial on a working tokamak. Furthermore, the above was calculated for "worst case" conditions. Even if these conditions exist presently, they are amenable to correction in the near future.

The conclusion is that the present Lyman-α scattering system operates within the anticipated boundaries. No unanticipated interferring effects have been noted and many of the anticipate effects have been reduced to inconsequential levels. Nevertheless, some of the optical alignments and through-put efficiencies must be brought up to higher standards before experiments on the main plamsa edge will be successful.

7. Lyman-α Production with the Argon Excimer Laser

7.1 The Argon Excimer Laser

Another possibility of getting high power at Lyman α is to try a direct laser operation in the VUV. Since the invention of the laser there have been numerous efforts to extend the spectral range of laser radiation. However, the development of lasers with wavelengths in the VUV spectral range is still in its infancy. The best performances to date have been achieved with rare gas excimer lasers. Of these the argon excimer laser is the one with the shortest wavelength. Hughes et al. /7/ did already achieve in 1974 lasing in argon at 126,1 nm. Because of its broad fluorescence spectrum the argon excimer laser is finding increased interest for being tuned to Lyman α.

To investigate the potential of an argon laser for Lyman-α production we set up a high power electron beam pumped excimer laser system. As electron gun we use a Pulserad 110 A with a peak current of 11 kA at a typical voltage of 1.3 MV. We build a coaxial diode similar to the diode first used by Bradley /8/. Up to 50 Joules are deposited in 5 cm^3 of argon gas at a pressure of 60 bar during a 20 ns electron beam pulse.

The anode tube, containing the gas, is made of stainless steel with an inner diameter of 5 mm and a wall thickness of 100 micrometer (Fig. 8). In order to suppress grazing incidence reflection from the tube walls, we inserted a wire spiral into the anode tube.

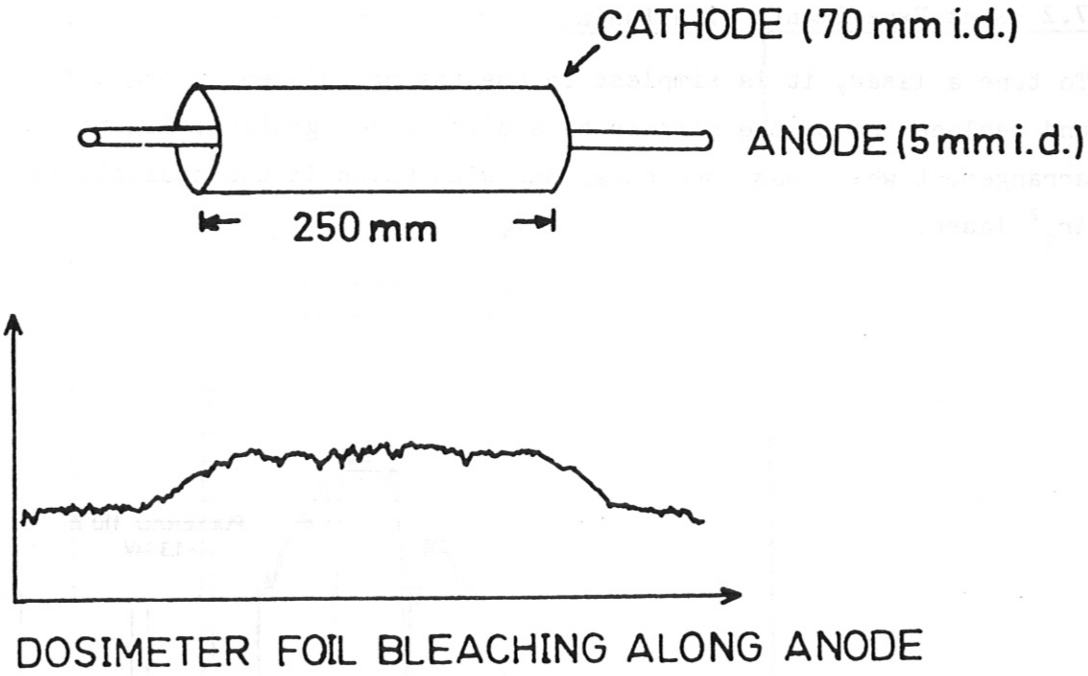

Fig. 8 Coaxial Diode and measurement of the measured homogeneity of the field emission discharge.

A concentric titanium cathode with a diameter of 70 mm pumps a 25 cm region. The electron energy deposition along the anode was measured by cellophane dye dosimetry. It is homogeneous throughout the cathode (s. Fig. 8).

The pressure chambers at the ends of the anode contain the laser mirrors. The cavity length is 50 cm. The vacuum ultraviolet radiation is transmittd by MgF_2 windows and then divided by a calibrated MgF_2 beam splitter onto a fast photodiode and the entrance slit of a McPherson 225 spectrograph (s. Fig. 9).

As the biggest problem with the Ar_2^* laser is damage to mirrors, experiments with absolutely resistive mirrors occupy a central role. Fortunately, with our high power excitation it is already possible to achieve lasing with two uncoated MgF_2 plates. The highest laser power at 126.1 nm was obtained with one 80 % reflectling mirror and one MgF_2 (5 % reflection) plate. Reproducible output power of 250 kW were reached at 33 bar. With an irradiated area of 0.2 cm^2 the damage threshold of the mirror is thus around 1.25 MW/cm^2 corresponding to an intracavity power of 250 kW.

7.2 Laser Experiments with Tuning

To tune a laser, it is simplest to use the principles of angular dispersion and replace one of the mirrors by a diffraction grating. Figure 9 shows the arrangement which was used here, and with which it was possible to tune the Ar_2^* laser.

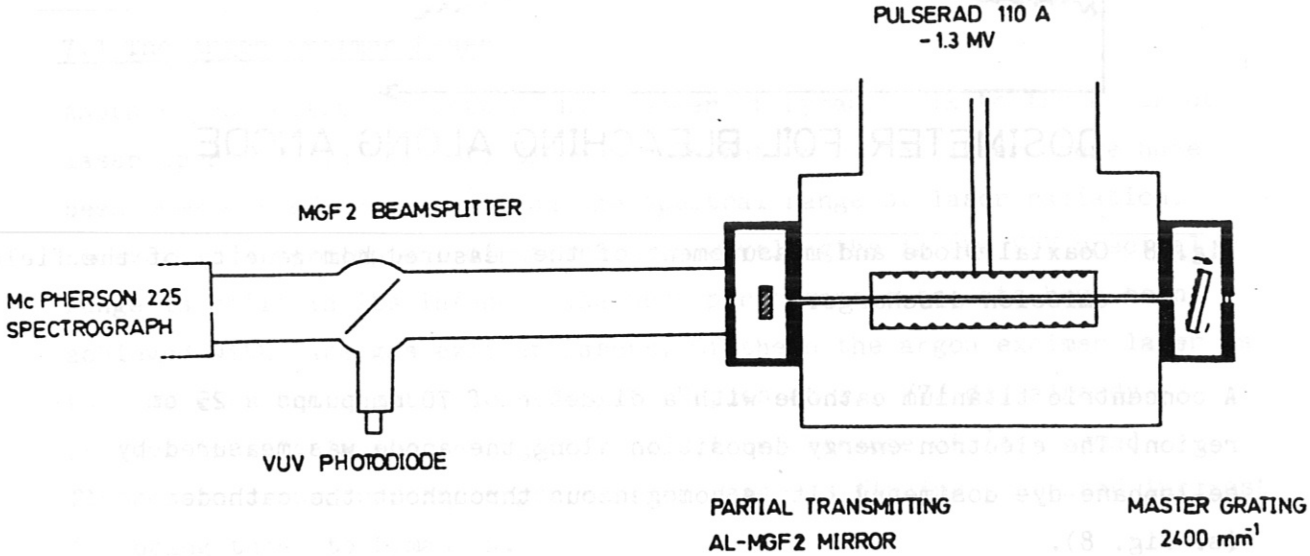

Fig.9 Experimental set-up. The 80 % mirror is replaced by a diffraction grating.

With the diffraction grating in the resonator the laser line width is 0.6 nm, which is nearly a factor of 3 smaller than the width of the untuned laser. Near impurity lines, the line width even decreases to 0.2 nm.

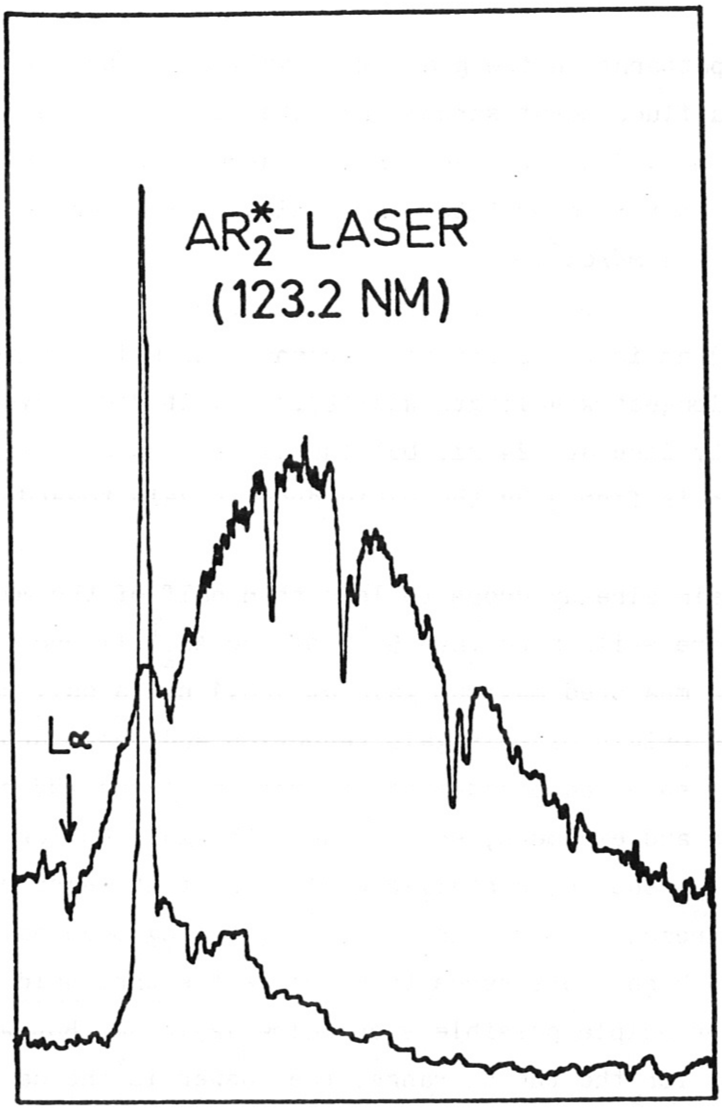

Fig. 10 Shortest wavelength laser line with tuning by grating; as comparison the fluorescence spectrum is also shown.

Figure 10 shows a tuned laser spectrum with the grating in the resonator. For comparison, we produced a fluorescence spectrum on the same strip of film. We fired many times on the same gas filling to produce deliberately impurity absorption lines, which we use for calibration.

In order to tune to Lyman alpha, gas impurities are a problem for the argon excimer laser, but in the present state of development, they are not the dominant one.
This is damage in optical coatings. The maximum laser signal that we measured, without the grating being damaged afterwards, correspods to 3 kW. This is equivalent to an intracavity laser intensity of about 200 kW/cm^2 - if we assume that the laser intensity is distributed homogeneously across the anode tube.

However, the burn patterns on the grating as well as visual observations of the laser beam on a fluorescent screen indicate that the laser beam has a smaller cross-section and a low divergence of about 5 mrad. We estimate its diameter in the resonator to be 2 to 3 mm. This means a damage threshold of the grating of about 1 MW/cm^2.

At the moment 123.2 nm is the shortest wavelength at which we achieved laser action. The longest wavelength was 127.4 nm. It did prove possible to overcome an impurity line at 124 nm, but the limit of tunability to even shorter wavelengths is formed by the rapid drop in gain towards Lyman α.

The small-signal gain already drops to less than half of the maximum value at a wavelength where still more than 50 % of the Ar_2^* fluorescence intensity is present. The measured maximum gain at 126.1 nm is only half of the expected value. The origin of this gain reduction and sharp drop towards Lyman-α is probably enhanced broad-band absorption of the VUV radiation by excited argon atoms and excimers, which reduce the gain to low values. Lasing in our cavity requires a small-signal gain of at least 0.07 cm^{-1}. When this value is reached at 25 bar at 126 nm, lasing occured. At smaller wavelengths we need higher pressures to overcome the threshold of 0.07 cm^{-1}, which is in principle possible even below 123.2 nm. But what is then the limiting factor for the tuning range; the answer is the damage of the grating by superfluorescence, which also increases with pressure. At higher pressures the amplified spontaneous emission around 126.1 nm is so strong that the grating was damaged without laser action. Also the use of MgF_2 or LiF prisms as dispersion elements instead of a grating is not useful to broaden the tuning range and the resulting power. In these cases the limiting factor is the damage of the partially transparent mirror.

<u>Summary: Tuning by Angular Dispersion</u>

The dispersive properties of the tuning elements are largely similar. This also applies to the experimental results, which can be summarized as follows

- it has been possible for the first time to tune the Ar_2^* laser. This makes it the tunable laser with the shortest wavelength.
- the tuning range extends from 123.2 nm to 128.4 nm (using MgF_2 prism).

- the line width is between 0.25 nm and 0.6 nm.
- the power is up to 3 kW.

The limited power is due to the sensitivity of the grating or partially transparent mirror which, however, is necessary to achieve tuning by angular dispersion. In order to produce sufficient gain still at the wings of the Ar_2^* continuum, the small-signal gain in the line center has to be raised so high that the superfluorescence destroy the mirror.

7.3 New Prospects

The electron-beam-pumped argon excimer laser is a powerful VUV light source at 126.1 nm. Failure of intracavity tuning to Lyman-α (121.6 nm) results from the low gain at 121.6 nm. However there exists the posibility to shift the Ar_2^*-laser line to Lyman-α by stimulated Raman scattering, if one uses the first order anti-Stokes line in deuterium.

To estimate the requirements of the Ar_2^*-laser with regard to power and luminosity necessary for an efficient Raman shifting to Lyman-α the stimulated Raman effect in different gases (H_2, D_2, CH_4) was investigated with a commercially available ArF-pump laser (193 nm). The results show that the minimum luminosities required for shifting the Ar_2^*-laser in deuterium exceeds those presently achievable by two orders of magnitude.

There is at present no hope of significantly increasing the luminosity of the available Ar_2^*-laser. This would require elongation of the effective resonator length. Limits are imposed, however, because the lifetime of the excimers is already in the region of the transit time of the light in the resonator.

Travelling wave excitation might be conceivable, but this would call for complete modification or reconstruction of the laser.

With further effort in this direction it may yet be possible to come up with a Lyman-α source based on a Raman-shifted argon excimer laser.

References

/1/ J. Neuhauser, K. Lackner, R. Wunderlich, Proc. Internat. Conf. on Plasma Physics 1982, Göteborg 12 BI:1.

/2/ D.W. Koopman, T.J. McKrath, V.P. Myerscough, J. Quant. Spectrosc. Radiat. Transfer, 19, 55 (1978).

/3/ C. Breton, R. Papoular, Report EUR-CEA-FC 728 (1974).

/4/ P. Bogen, Y.T. Lie, Appl. Phys. 16, 139 (1978).

/5/ H. Langer, IPP Report 1/185 (1981).

/6/ P. Bogen, R.W. Dreyfus, Y.T. Lie, H. Langer, to be published in Journal of Nuclear Materials (Int. Cont. of plasma wall interaction 1982, Gatlinburg).

/7/ W.M. Hughes, J. Shannon, R. Hunter, Appl. Phys. Lett. 24 (1974), 488.

/8/ D.J. Bradley, D.R. Hull, M.H.R. Hutchinson, M.W. McGeoch, Opt. Comm. 11 (1974) 335.